Extension of Global Gyrokinetic Code for Tokamak Edge Turbulence Simulation*)

Shuhei OKUDA, Haruki SETO[1)] and Kenji IMADERA

Graduate School of Energy Science, Kyoto University, Uji 611-0011, Japan

[1)]*Rokkasho Fusion Institute, National Institutes for Quantum Science and Technology, Rokkasho 039-3212, Japan*

(Received 4 January 2023 / Accepted 15 March 2023)

A field-aligned coordinate system using a shifted metric technique has been implemented to a global gyrokinetic code GKNET. This coordinate system allows for simulations with lower resolution in the direction along the magnetic field line, which is especially effective in the outer core regions with higher q values. Realistic tokamak geometries, including up-down asymmetric equilibria, have also been implemented by using a newly developed interface code that connects GKNET and a free-boundary 2D Grad-Shafranov equation solver. This is essential for tokamak edge simulations, which will be developed in the future. As an application, the nonlinear simulation of the ion temperature gradient (ITG) mode with the JT-60SA ITER-like plasma [M. Nakata *et al.*, Plasma Fusion Res. **9**, 1403029 (2014)] has been performed. The result shows that the linear ITG instability with high poloidal modes and resultant zonal flow generation are properly traced. In this case, it is estimated that the number of computational grids can be reduced to 1/94 compared to that of the flux surface coordinate system.

Keywords: global gyrokinetic code, field-aligned coordinate, realistic geometry, JT-60SA plasma, ITG mode, nonlinear simulation

DOI: 10.1585/pfr.18.2403040

1. Introduction

The dynamics of plasma in the tokamak edge, particularly in the outer core region that connects with the SOL/divertor region, is crucial for several aspects such as fuel supply/impurity pumping, divertor heat load control, L-H transition, and others. These issues are particularly important for upcoming fusion devices like JA-DEMO [1]. Although gyrokinetic simulation is an essential tool for studying these physics based on the first principle, it is challenging to apply it to the edge region due to higher q values and complex magnetic surface geometries that are not present in the core region.

To address these problems, we have implemented a field-aligned coordinate system [2] using a shifted metric technique [3] into our global gyrokinetic code GKNET [4]. This system can significantly reduce the computational cost because the wavenumbers of resonant instabilities are low in the direction along the magnetic field lines. It is especially useful in edge regions where higher poloidal mode numbers resonate with the higher q values.

We have also developed an interface code that connects GKNET with a free-boundary 2D Grad-Shafranov equation solver. This integration allows for gyrokinetic simulations with realistic tokamak equilibria, including up-down asymmetric equilibria that cannot be handled by the conventional GKNET [5].

The paper is organized as follows. Section 2 explains the field-aligned coordinate system and the correction of its secular cell deformation using the shifted metric technique. Section 3 provides the calculation model used in the study with GKNET. Section 4 presents a linear simulation of the ion temperature gradient (ITG) mode in a concentric circular torus plasma with cyclone-base-case (CBC) parameters. Section 5 presents a nonlinear simulation of ITG mode in a JT-60SA plasma. Finally, Sec. 6 provides a summary of the findings and outlines future plans.

2. Field-Aligned Coordinate System

A field-aligned coordinate system [2] is a coordinate system, in which one of the covariant basis vectors is chosen along the magnetic field line. This system can significantly reduce computational cost because the wavenumbers of resonant instabilities are low in the direction along the magnetic field line. However, this coordinate system often has a secular cell deformation, which can degrade the accuracy of the radial differences in the finite difference method.

In this paper, we use field-aligned coordinates that utilizes the poloidal angle as the label along the magnetic field line. We employ a shifted metric technique [3] to correct the secular cell deformation. The shifted metric method technique divides the torus into N_s segments with respect to the poloidal angle and defines field-aligned coordinates with an appropriate reference point as $\theta_j = -\pi + 2\pi(j + 0.5)/N_s$ in each segment, where $j = 0, 1, \cdots, N_s - 1$. In

author's e-mail: okuda.shuuhei.38z@st.kyoto-u.ac.jp

*) This article is based on the presentation at the 31st International Toki Conference on Plasma and Fusion Research (ITC31).

this case, the field-aligned coordinates in the j-th segment (x_j, y_j, z_j) are defined as:

$$x_j = \rho, \tag{1}$$
$$y_j = y_{\mathrm{shift},j} - \zeta, \tag{2}$$
$$z_j = \theta - \theta_j, \tag{3}$$

where the shift angle $y_{\mathrm{shift},j}$ is defined with the magnetic field pitch $\nu \equiv (\boldsymbol{B}\cdot\nabla\zeta)/(\boldsymbol{B}\cdot\nabla\theta)$,

$$y_{\mathrm{shift},j}\,(x,z) = \int_{\theta_j}^{\theta} \nu(\rho,\theta')\mathrm{d}\theta'. \tag{4}$$

Here, ρ is a radial coordinate that corresponds to a magnetic-flux-surface, while θ and ζ represent the arbitrary poloidal and geometrical toroidal angles, respectively. The unit vector parallel to the magnetic field and the parallel gradient can be expressed as:

$$\boldsymbol{b} \equiv \frac{\boldsymbol{B}}{|\boldsymbol{B}|} = \frac{1}{\sqrt{g_{zz}}}\boldsymbol{e}_z, \quad \nabla_\parallel \equiv \boldsymbol{b}\cdot\nabla = \frac{1}{\sqrt{g_{zz}}}\frac{\partial}{\partial z}, \tag{5}$$

where $\boldsymbol{e}_z$ is the covariant basis vector for z and $g_{zz} \equiv \boldsymbol{e}_z\cdot\boldsymbol{e}_z$ is the zz component of the covariant metric tensor. It is important to note that this analysis assumes toroidal axisymmetric equilibria.

The computational domain of the N_w-th annular wedge torus is represented by N_s segments defined in the following range,

$$L_x \in [x_a,\ x_b]\,,\ L_y \in \left[0,\ \frac{2\pi}{N_w}\right),\ L_z \in \left[-\frac{\pi}{N_s},\ \frac{\pi}{N_s}\right). \tag{6}$$

Here, N_w denotes the wedge number, x_a and x_b indicate the inner and outer boundaries of radial domain, and the field-aligned girds (y, z) in the (θ, ζ)-plane for $N_s = 1$ and $N_s = 4$ are shown in Figs. 1 and 2, where $N_w = 1$.

In this coordinate system, the position along the magnetic field line is labeled by the poloidal angle. Compared to the flux surface coordinates (ρ, θ, ζ), it is particularly effective in the edge regions where the higher poloidal mode numbers resonate with the higher q values because the spatial domain is discretized in the direction aligned with the field line instead of the poloidal direction.

The wavenumber in the x direction is written as

$$k_x = k_\rho + n\int_{\theta_j}^{\theta} \frac{\partial\nu(\rho,\theta')}{\partial\rho}\mathrm{d}\theta', \tag{7}$$

where n is the toroidal mode number. There are regions where $|k_x| > |k_\rho|$ due to the second term in Eq. (7), which requires higher resolution in the radial direction. This is a significant problem, particularly in edge regions where the magnetic shear is higher and the higher toroidal mode numbers resonate. Increasing N_s can alleviate this problem by reducing the integral interval of the second term in Eq. (7) in each segment as is shown in Fig. 2.

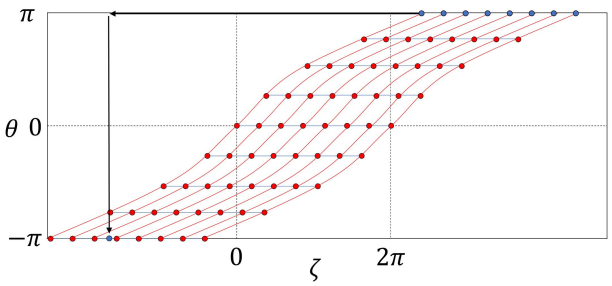

Fig. 1 Computational grids of (y, z) for $N_s = 1$ on a flux surface. The red and blue lines indicate the y- and z- directions respectively. Arrows indicate double periodic boundaries.

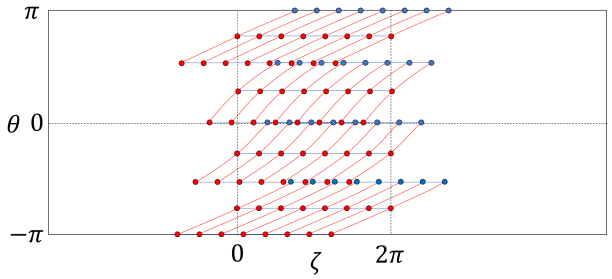

Fig. 2 Computational grids of (y, z) with the shifted metric for $N_s = 4$ on a flux surface. The blue dots are the buffer cell (note that only a part is shown).

To interpolate physical quantities between segments, we employ coordinate transformation via phase relations. Let us consider the coordinate transformation of a quantity a from the j-th segment $a(x_j, y_j, z_j)_j$ to $j+1$-th segment $a(x_{j+1}, y_{j+1}, z_{j+1})_{j+1}$. The Fourier series expansion of $a(x_j, y_j, z_j)_j$ with respect to the toroidal mode number n, in in the j-th segment, can also be expressed in the $j+1$-th segment.

$$\begin{aligned} &a(x_j, y_j, z_j)_j \\ &\quad= \sum_n \hat{a}_n(x_j, z_j)_j \exp(\mathrm{i}n y_j), \\ &\quad= \sum_n [\hat{a}_n(x_j, z_j)_j \exp(-in\Delta_{\mathrm{shift}})] \exp(\mathrm{i}n y_{j+1}), \end{aligned} \tag{8}$$

which results in

$$\hat{a}_n(x_{j+1}, z_{j+1})_{j+1} = \hat{a}_n(x_j, z_j)_j \exp(-in\Delta_{\mathrm{shift}}). \tag{9}$$

Here, Δ_{shift} is the relative phase shift,

$$\Delta_{\mathrm{shift}} = y_{\mathrm{shift},j+1} - y_{\mathrm{shift},j} = -\int_{\theta_j}^{\theta_{j+1}} \nu\,(\rho,\theta')\mathrm{d}\theta'. \tag{10}$$

Using Eq. (9) for interpolation in Fourier space provides a very smooth connection between segments.

3. Calculation Model in GKNET

The GKNET code is a global gyrokinetic code that evolves the perturbed gyro-center distribution function of

each particle species and the perturbed electrostatic potential by self-consistently solving the gyrokinetic Vlasov equation and the gyrokinetic quasi-neutrality condition.

In this study, bulk ions are assumed to be protons. The collisionless electrostatic gyrokinetic Vlasov equation for ions can be expressed as follows:

$$\frac{\partial \delta f}{\partial t} + \boldsymbol{V}_{\boldsymbol{R}}^{(0)} \cdot \nabla \delta f + \boldsymbol{V}_{\boldsymbol{R}}^{(1)} \cdot \nabla f_0 + \boldsymbol{V}_{\boldsymbol{R}}^{(1)} \cdot \nabla \delta f + V_{v_\parallel}^{(0)} \frac{\partial \delta f}{\partial v_\parallel} + V_{v_\parallel}^{(1)} \frac{\partial f_0}{\partial v_\parallel} + V_{v_\parallel}^{(1)} \frac{\partial \delta f}{\partial v_\parallel} = 0, \tag{11}$$

with

$$\boldsymbol{V}_{\boldsymbol{R}}^{(0)} = \frac{1}{B_\parallel^*} \left(\boldsymbol{B}^* v_\parallel + \frac{1}{e} \boldsymbol{b} \times \nabla H^{(0)} \right), \tag{12}$$

$$\boldsymbol{V}_{\boldsymbol{R}}^{(1)} = \frac{1}{B_\parallel^*} \left(\frac{1}{e} \boldsymbol{b} \times \nabla H^{(1)} \right), \tag{13}$$

$$V_{v_\parallel}^{(0)} = -\frac{1}{m_i B_\parallel^*} \boldsymbol{B}^* \cdot \nabla H^{(0)}, \tag{14}$$

$$V_{v_\parallel}^{(1)} = -\frac{1}{m_i B_\parallel^*} \boldsymbol{B}^* \cdot \nabla H^{(1)}, \tag{15}$$

where the gyro-center distribution function of ions f is scale-separated by the gyrokinetic ordering, as given by: $f(\boldsymbol{R}, v_\parallel, \mu, t) = f^{(0)}(\boldsymbol{R}, v_\parallel, \mu) + f^{(1)}(\boldsymbol{R}, v_\parallel, \mu, t) = f_0(\boldsymbol{R}, v_\parallel, \mu) + \delta f(\boldsymbol{R}, v_\parallel, \mu, t)$, where f_0 represents the equilibrium part of f given by the local Maxwellian distribution function $f_0 = f_M$, δf represents the perturbed part of f. $H^{(0)} = \frac{1}{2} m_i v_\parallel^2 + \mu B$ and $H^{(1)} = e\langle \phi \rangle$ are the zeroth and the first-order of the gyrokinetic Hamiltonian, respectively. Here, $\langle \cdots \rangle$ represents the gyro-averaging operator, $\boldsymbol{B}^* \equiv \boldsymbol{B} + \frac{m_i}{e} v_\parallel \nabla \times \boldsymbol{b}$ and $B_\parallel^* \equiv \boldsymbol{B}^* \cdot \boldsymbol{b}$. It is worth noting that $(\boldsymbol{R}, v_\parallel, \mu)$ are the gyro-center coordinates. where $\boldsymbol{R}$ is the gyro-center position, $v_\parallel$ is the parallel velocity and μ is the magnetic moment defined by $\mu \equiv m_i v_\perp^2 / 2B$ with the perpendicular velocity $v_\perp$.

The gyrokinetic quasi-neutrality condition, with adiabatic electron response is expressed as follows:

$$\nabla_\perp \cdot \left(\frac{m_i n_0}{B^2} \nabla_\perp \phi \right) - \frac{e^2 n_0}{T_e} \left(\phi - \langle \phi \rangle_f \right) = -2\pi \frac{e}{m_i} \iint \langle \delta f B_\parallel^* \rangle \, \mathrm{d}v_\parallel \mathrm{d}\mu, \tag{16}$$

where ϕ is the electrostatic potential and $\langle \cdots \rangle_f$ is the flux-surface-averaging operator.

The physical quantities are normalized by the magnetic field strength at the magnetic axis B_0, the ion temperature at the half minor radius T_{i0}, the density at the half minor radius n_0, the elementary charge e, the ion mass m_i, the thermal velocity $v_{ti} = \sqrt{T_{i0}/m_i}$, the ion cyclotron frequency $\Omega_i = eB_0/m_i$, and the gyro radius $\rho_{ti} = v_{ti}/\Omega_i$.

The computational domain is represented by

$$L_{v_\parallel} \in [-v_c,\ v_c]\,,\ L_\mu \in [0,\ \mu_c]\,, \tag{17}$$

in addition to Eq. (6), where v_c and μ_c are the normalized cut-off velocity and magnetic moment, respectively.

In this work, Dirichlet boundary conditions are set at the inner and outer radial boundaries, such that:

$$\delta f(x = x_a) = \delta f(x = x_b) = 0. \tag{18}$$

4. ITG Simulation with Concentric Circular Torus

To verify the GKNET code using the field-aligned coordinates with the shifted metric, a linear ITG simulation is performed with the CBC parameters in a concentric circular torus.

The simulation is set up as follows: The GKNET code considers gyrokinetic ions and adiabatic electrons. The radial coordinate is defined as $x = r/a_0$ where r is the geometrical minor radius and a_0 is the minor radius at the last closed flux surface. The range of the simulation domain is set to $L_x \in [0.1,\ 1]$ to exclude the magnetic axis. The normalized cut-off velocity and magnetic moment are set to $v_c = 5$, $\mu_c = 12.5$, respectively. The number of grids used for this simulation are $(N_x, N_y, N_z, N_{v_\parallel}, N_\mu) = (128, 216, 32, 80, 16)$ for both $N_s = 1$ and $N_s = 8$. The time increment used is $\Delta t\, v_{ti}/R_0 = 1/100$. The system size is $a_0/\rho_{ti} = 150$ and the parameters $a_0/R_0 = 0.36$, $R_0/L_n = 2.22$, $R_0/L_{T_i} = R_0/L_{T_e} = 6.92$, $q = 0.85 + 2.18(r/a_0)^2$ are set, where R_0 is the major radius at the magnetic axis. The regions with steep density/temperature gradients are centered at $r/a_0 = 0.5$ and the magnetic shear $s = r/q\, \mathrm{d}q/\mathrm{d}r$ is small at $r/a_0 = 0.5$. Consequently, the cell deformation is expected to be small, and there is little difference expected between the simulation results obtained with $N_s = 1$ and those obtained with $N_s = 8$.

Figure 3 demonstrates that the linear growth rates are nearly identical for both $N_s = 1$ and $N_s = 8$, which suggests that the implementation of the field-aligned coordinate system with the shifted metric is successful.

5. ITG Simulation with JT-60SA ITER-like Equilibrium

In addition to the development of the interface code that connects GKNET with a free-boundary 2D Grad-Shafranov equation solver, we present a result of a non-

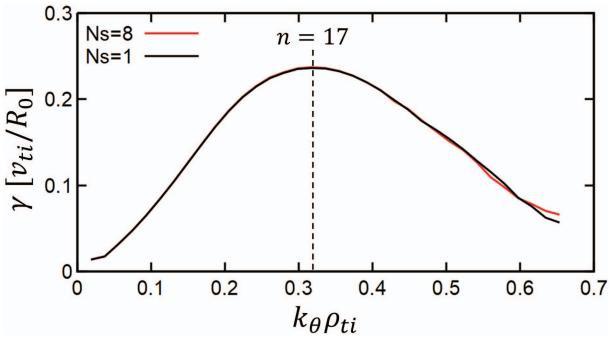

Fig. 3 Dispersion relations of toroidal ITG instability in the CBC case for $N_s = 1$ (black) and $N_s = 8$ (red).

linear electrostatic ITG simulation with δf global model in a JT-60SA ITER-like plasma [6].

The simulation set up is as follows: gyrokinetic ions and adiabatic electrons are considered. The system size is $a_0/\rho_{ti} = 294$. The radial coordinate is defined by $x = \rho = \sqrt{\psi}$ where ψ is the normalized poloidal magnetic flux function defined with $\psi = 0$ at the magnetic axis and $\psi = 1$ at the separatrix. $L_x \in [0.1,\ 0.9]$ is set to remove the magnetic axis and the pedestal region. The domain of the velocity space is the same as in Sec. 4. The numbers of grids are $(N_x, N_y, N_z, N_{v_\parallel}, N_\mu) = (720, 256, 32, 80, 16)$ and the number of segments in the shifted metric is $N_s = 8$, where the wedge number is $N_w = 4$. The time increment is $\Delta t\ v_{ti}/R_0 = 1/100$. Figure 4 shows the profiles of this equilibrium, where $T_i = T_e$. This result demonstrates the successful implementation of the interface code, allowing GKNET to handle realistic tokamak equilibria. In Fig. 5, we present the dispersion relation and poloidal harmonics of the $n = 100$ component of electrostatic potential $e\phi_{n=100}/T_{i0}$, which is the most unstable mode, in the linear simulation. The dispersion relation is qualitatively consistent with the previous research that used a local gyrokinetic code [6]. We observe that the resonance condition $m = nq$ is satisfied for $(m, n) = (233, 100)$ with $q = 2.33$. In Fig. 6, we show the linear growth of initially unstable modes and their nonlinear saturation. Figure 7 confirms that the linear instability with the high poloidal mode is resolved, and the zonal flow is generated at the corresponding locations.

Finally, we discuss the number of grids required. We consider the poloidal grids required to resolve $n = 160$ and $m_{\rm res} = nq = 160 \times 2.3 \approx 370$ mode, which is unstable in this case. Assuming that 8 times the number of grids are

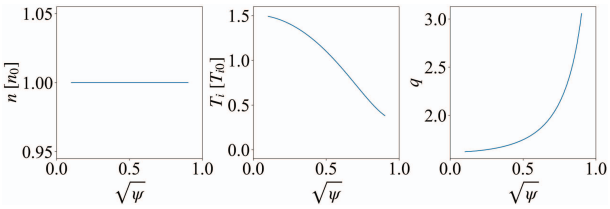

Fig. 4 Profiles of JT-60SA ITER-like equilibrium in this study.

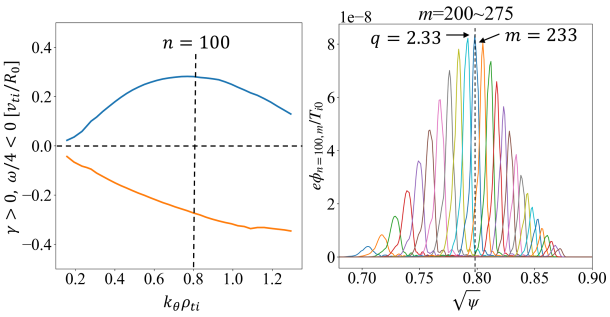

Fig. 5 Dispersion relations (left) of toroidal ITG mode and the poloidal harmonics of $e\phi_{n=100}/T_{i0}$ (right) in the linear simulation.

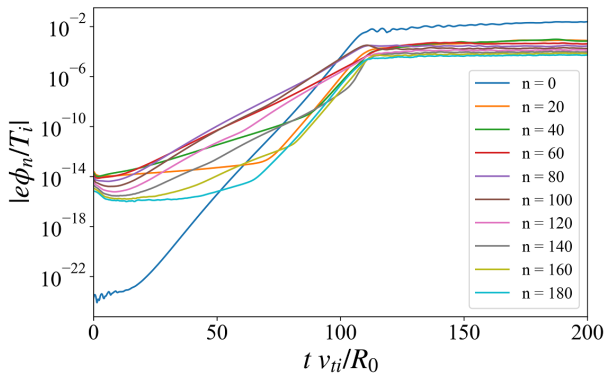

Fig. 6 Time evolution of the toroidal mode energy $|e\phi_n/T_{i0}|$. Note that they are averaged over the poloidal cross section.

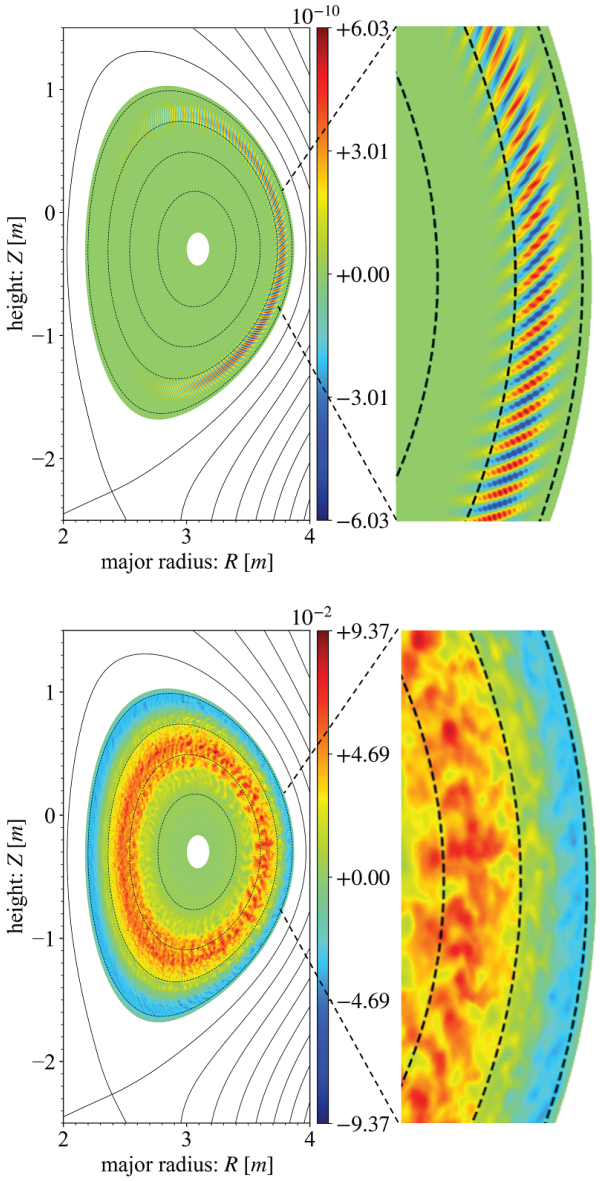

Fig. 7 $\mathrm{Re}(e\phi_{n=100}/T_{i0})$ in the linear phase at $t\ v_{ti}/R_0 = 50$ (up) and ϕ ($\zeta = 0$) after the nonlinear saturation at $t\ v_{ti}/R_0 = 200$ (down).

needed for the mode number, $N_\theta = 370 \times 8 \approx 3000$ grids are required when using flux surface coordinates (ρ, θ, ζ). On the other hand, when using the field-aligned coordinates (x, y, z), only $N_z = 32$ grids are sufficient, as in this case. Therefore, it is estimated that the number of required grids can be reduced to $32 \div 3000 \approx 1/94$ by using the field-aligned coordinate system.

6. Summery and Future Plans

The field-aligned coordinate system has been successfully implemented into the global gyrokinetic code GKNET to effectively address instabilities with high poloidal mode numbers, which were previously difficult to handle using cylindrical coordinates (R, Z, ζ) or flux surface coordinates (ρ, θ, ζ). The implementation of this system, with the shifted metric, has been validated by performing the ITG simulation with the concentric circular torus.

Furthermore, the development of an interface code that connects GKNET with a free-boundary 2D Grad-Shafranov equation solver, has enabled the handling of realistic tokamak equilibria, including up-down asymmetric equilibria which was not possible with earlier versions of GKNET.

A nonlinear ITG simulation has been carried out on the JT-60SA ITER-like plasma, demonstrating that the linear instability of the high poloidal mode number has been resolved and that the corresponding zonal flow has been generated. The use of the field-aligned coordinate system has resulted in a significant reduction of computational grids, estimated to be approximately 1/94 in comparison to the flux surface coordinate system.

In future plans, the development of GKNET will be extended to address tokamak edge turbulence. Currently, an interface code is being developed to generate a computational grid of field-aligned coordinates in the SOL/divertor region, initially focusing on an electrostatic model before investigating the important issues discussed in the introduction.

Acknowledgments

The authors would like to express their gratitude to Dr. Nobuyuki Aiba for generously providing the JT-60SA equilibrium data.

The simulations were conducted on JFRS-1 in IFERC-CSC and the Plasma Simulator in NIFS. This work was supported by the JSPS KAKENHI Grant Number 20K03903 and the Joint Special Design Team Collaborative Research Program (31K031).

[1] K. Tobita *et al.*, Fusion Sci. Tech. **75**, 372 (2019).
[2] M.A. Beer *et al.*, Phys. Plasmas **2**, 7 (1995).
[3] B. Scott, Phys. Plasmas **8**, 447 (2001).
[4] K. Imadera *et al.*, Proc. 25th FEC, TH/P5-8 (2014).
[5] K. Imadera *et al.*, Plasma Fusion Res. **15**, 1403086 (2020).
[6] M. Nakata *et al.*, Plasma Fusion Res. **9**, 1403029 (2014).